TITLE: Ion Trapping in the Virtual Cathode of the Penning Fusion eXperiment-Ions

Ion Trapping in the Virtual Cathode of the Penning Fusion eXperiment-Ions

M. M. Schauer, D. C. Barnes, K. R. Umstadter [*]

Los Alamos National Laboratory, Los Alamos,NM 87545, USA

Abstract. The goal of the Penning Fusion eXperiment-Ions (PFX-I) is the production of thermonuclear conditions in a Penning trap by means of spatial and/or temporal compression of a high temperature plasma. The present approach involves the confinement of positive ions in a virtual cathode produced by a nonthermal electron plasma held within a modified Penning trap. We report here on the first evidence of ions trapped in three dimensions in this manner. Experimental evidence of the maintenance of the non-Maxwellian electron energy distribution needed to produce the virtual cathode is presented.

We utilize the excellent confinement times achieved with Penning traps [1] for confining thermonuclear plasmas. For a practical value of reactivity, it is necessary to enhance the rms density beyond limitations imposed by the nonneutrality of the trapped plasmas. The density of a uniform, nonneutral plasma confined in a Penning trap is limited to the Brillouin limit [2] set by the balance between the repulsive force of the space charge of the plasma and the restoring force provided by its rotation in the external magnetic field.

However, focusing the orbits of the constituent particles can produce a nonuniform plasma with an enhanced density over some small volume. Indeed, enhanced densities, inferred to significantly exceed the Brillouin limit, have been demonstrated in a pure electron plasma [3, 4]. Focusing was achieved in these experiments by injecting low angular momentum electrons into trapping fields tuned so that the period of the motion in the radial plane is twice that of the motion along the trap axis. Hence, any orbit originating at the trap center was necessarily constrained to pass through the center again. In essence, a Penning trap operated in this manner can be thought of as an inertial electrostatic confinement (IEC) [5, 6] device where the vacuum fields of the trap replace the grids of a standard IEC machine. Since the grids constitute the chief source of particle and energy loss in most IEC experiments, this approach greatly improves confinement.

A limitation of this approach is that the axial and radial frequencies of motion depend differently on the charge-to-mass ratios of the constituent particles. Therefore, unlike IEC, this method only works for plasmas with a single charge-to-mass ratio, such as pure deuterium plasmas, and is not applicable to those systems offering the highest fusion cross sections, i.e. mixed deuterium and tritium plasmas.

One system that offers the possibility of focusing independent of the charge-to-mass ratio of the confined species is a spherically symmetric virtual cathode produced within a trapped electron plasma. Here, the potential providing ion confinement is produced by the space charge of the trapped electron cloud and is spherically symmetric, thereby ensuring that the confining force experienced by the ions is purely radial regardless of their charge-to-mass ratio. This configuration has the added advantage that, if the con-

CP606, *Non-Neutral Plasma Physics IV*, edited by F. Anderegg et al.

fining potential is harmonic, i.e. produced by a uniform density electron cloud, in addition to being spherically symmetric, then implementation of such temporal compression schemes as the proposed periodically oscillating plasma sphere (POPS) is also possible. Theoretical work on POPS indicates the possibility of compression ratios as high as 1500:1, albeit in single species plasmas [7, 8].

Radial confinement of positively charged ions by the negative space charge of an electron beam has been routinely accomplished in the electron beam ion trap or EBIT apparatus, although radial trapping is also provided by the applied magnetic field [9, 10, 11]. In those experiments a high current electron beam makes a single pass through the experiment and provides confinement in the direction perpendicular to the beam axis. Electrodes held at positive, static voltage provide axial confinement. This EBIT technology is not directly applicable in the present situation, because the desired thermonuclear ion energy and reasonably high electron density requires very high electric fields be applied near the desired ion well volume. These high fields are incompatible with the separately powered electrodes used to produce the EBIT axial well. Additionally, the high electron energy and density imply very high total electron current, which is very difficult to produce in a single-pass electron device, such as EBIT.

An alternative technology, appropriate for the desired thermonuclear application is adopted here. A virtual cathode is formed within a single conductor by an electron beam which achieves high total current by a large recirculation fraction. That is, a very low source of electron current is reflected many times between two cathodes which provide axial electron confinement. Radial electron confinement is provided by an applied magnetic field of up to 2 T. An axial well results from the shape of the anode cavity through which this beam passes. Furthermore, this well may be shaped by producing an axial gradient of the guiding magnetic field, although this design feature has not been implemented in the results presented here.

In this letter we give a first report on confinement of positive ions in a virtual cathode produced by a recirculating electron beam held in the Penning fusion experiment-ions (PFX-I). Here, axial confinement of ions is provided exclusively by the space charge of the recirculating electrons, while radial confinement is provided by the beam space charge and a 2T applied magnetic field. These results represent a first step towards the ion focusing goal as the virtual cathode is produced by a recirculating electron beam, however no focusing of the orbits of either the trapped electrons or ions was attempted.

Unlike standard harmonic Penning traps, the PFX-I electrodes are not hyperboloids of revolution, although they do possess cylindrical symmetry. The upper endcap (UEC) consists of a metal cap that contains an independently biased BaO electron emitter. The lower endcap (LEC) is made of $\approx$50% reflective grid formed from Molybdenum wire and can be held at constant voltage or discharged to ground externally through a 500 kΩ resistor ($\tau \sim 130\mu s$) to enable destructive measurement of the trapped particle inventory. The ring electrode has a 2 mm diameter hole passing through it with a diamond-shaped void machined into the midplane ($ID \approx 9mm$). Located below the trap are independently biased upper (UDT) and lower drift tubes (LDT) and a floating microchannel plate detector (MCP) which can be used together to detect and energy analyze particles ejected from the bottom of the trap when the LEC is discharged. Figure 1 is a schematic of the device.

To trap electrons both endcaps are held at negative potential, and the ring electrode is

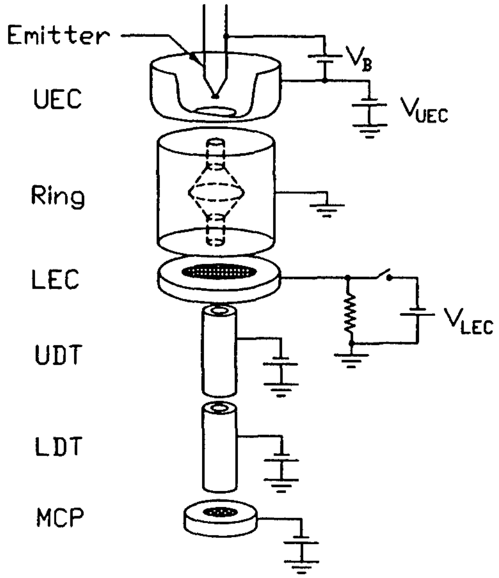

FIGURE 1. PFXI trap schematic. Figure is not to scale.

held at zero potential. The emitter is biased slightly positively (V_B=0.5V) with respect to the UEC, and electron emission is enabled by penetration from the trapping field. The LEC is biased 50V more negatively than the UEC (V_{LEC}=-550V and V_{UEC}=-500V), so the electron beam is reflected back upon itself. With this emitter bias configuration, the depth of the axial well for electrons increases with increasing radial distance. Beam electrons drift outward radially into the deeper axial well due to field inhomogeneities and collisions with neutral background gas molecules, hence reflexing many times in the trap before being lost to the ring electrode.

The entire apparatus is housed inside a room temperature vacuum system with base pressure of approximately 2×10^{-6} Pa. Residual gas analyzer spectra show the background gas to be $\geq 97\%$ H_2, and it is therefore assumed that any positive ions detected in the experiment are hydrogen ions. The vacuum system inserts into the warm bore of a superconducting magnet. The applied magnetic field was 2T for the measurements reported here.

The void in the midplane of the ring enables production of the virtual cathode when a nonthermal, i.e. beam-like, electron plasma is introduced into the trap. Neglecting end effects at the entrance and exit apertures, the potential within the grounded ring is uniform when no electron beam is present. Therefore, no confining fields exist. When a uniform density, electron beam is injected into the ring, the potential at the center of the void is now lower than within the entrance and exit channels. This can be seen by noting that the separation of an electron and its image charge is larger in the midplane of the ring than the corresponding separation in the entrance or exit channels. The resulting potential gradient provides axial confinement for positively charged particles.

It is important to note that production of a virtual cathode of significant strength

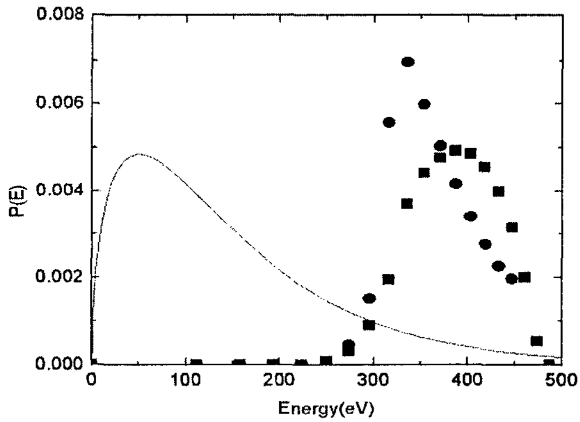

FIGURE 2. Energy spectra of the trapped electrons at 500 μs (boxes) and 25 ms (circles). The solid line is a three-dimensional Maxwellian distribution with kT=50 eV for comparison purposes only.

requires an electron cloud with a nonthermal energy distribution [12, 13]. A plasma in thermal equilibrium will merely rearrange itself to cancel out any external electric fields yielding, at best, a field free region incapable of confining positive ions. Such a nonthermal distribution can be maintained in a Penning trap if the time for relaxation to thermal equilibrium is longer than the plasma confinement time.

We find this to be the case in PFX-I. By measuring the total electron inventory as a function of the delay between the termination of electron beam injection into the trap volume and the discharge of the LEC, we find the 1/e time for the plasma inventory to be approximately 30 ms. Although no direct measurement of the equilibration time has been made, we calculate an electron-electron collision time ranging from 45 ms to 80 ms for electron energies from 300 eV to 500 eV. This calculation assumes a constant density of 3.2×10^9 cm^{-3} based on the initial inventory, i.e. 500 μs delay, of 5.8×10^8 electrons filling the entire trap volume from the LEC to the UEC.

Measurements of the electron energy distribution confirm the non-Maxwellian nature of the trapped electron plasma. Energy spectra were taken by measuring the electron inventory as a function of a negative bias voltage applied to the lower drift tube (LDT). All electrons with energy below this bias voltage were reflected and lost to the LEC grid rather than being counted by the MCP. A third order polynomial was then fitted to the data, and the derivative of this curve yielded the desired spectrum. Figure 2 shows typical spectra at 500 μs and 25 ms. Although it is difficult to make definitive statements about the form of the electron energy distribution, it is clearly non-Maxwellian, and the electron plasma can be said to be far from thermal equilibrium, consistent with the measured confinement time and calculated collision time.

A self-consistent solution of the electrostatic problem for a strongly-magnetized electron beam with these observed parameters confirms that an electrostatic ion well of significant depth should be formed within the anode cavity. The electron density is $n_e = R(r)F(\phi)$, where r is the cylindrical radius and ϕ the electrostatic potential, and R and F functions determined by the radial and parallel energy distribution of electrons,

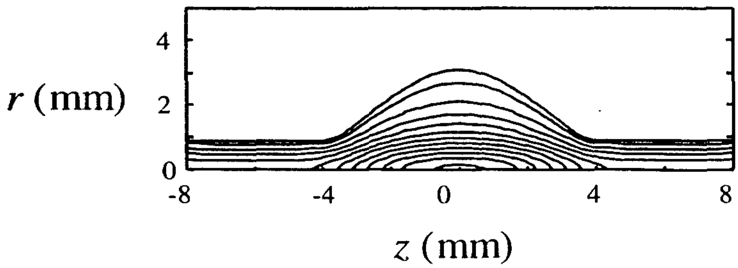

(a)

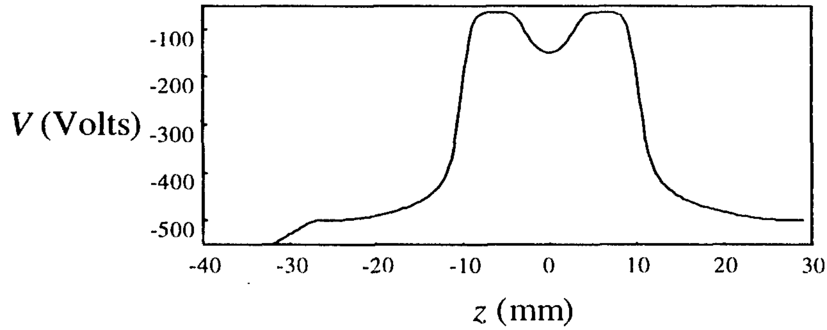

(b)

FIGURE 3. a)Theoretical contours of electrostatic potential in true perspective within the ring from the electrostatic solution. Dimensions are in mm. Central potential is - 176V, while ion well depth is 100V. b)On-axis potential diagram of the trap from UEC to LEC.

respectively. To describe the PFX-I electron configuration, it is assumed that R is determined by a uniform source over 1/2 the emitter tip radius and that the cross-B transport of electrons is independent of r. F is determined by assuming a uniform energy distribution of electrons between 300 eV and 500 eV.

A solution with the exact PFX-I electrostatic geometry has been found. Electron inventory is adjusted until the axial electric field near the UEC vanishes. This gives a value of 1.6×10^9 electrons, consistent with the observed inventory given the uncertainties in the absolute calibration of the electron collection efficiency and the approximations of the model used for the calculation. The electrostatic potential within the anode cavity is shown in Fig. 3(a). This electron-only solution gives an ion well of 20% of the applied voltage, or 100 V in the case under consideration.

Trapped ion space charge modifies this well depth prediction. Depending upon f_i, the ratio of the average ion density to the average electron density, this modification ranges from a small reduction of the well depth ($f_i \approx 0$) to nearly complete loss of the well ($f_i \approx 1$). Details of the ion source distribution and ion heating mechanisms determine f_i. Ultimately, one hopes to achieve $f_i \approx 0.1$ by tailoring the ion source and applying resonant ion heating.

Following confirmation of the non-Maxwellian nature of the electron distribution, the bias voltages applied to the LDT and MCP were set to negative 750V and negative

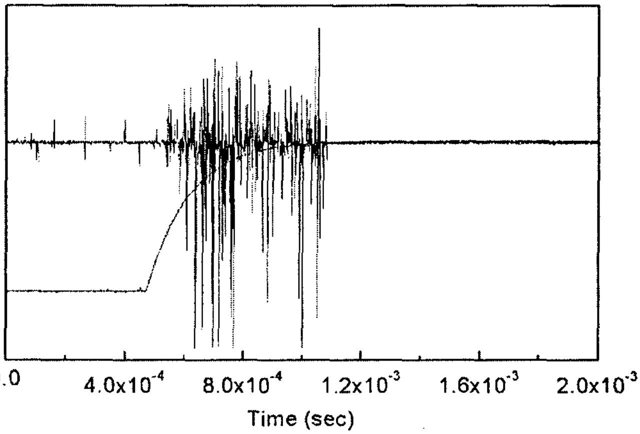

FIGURE 4. MCP output and LEC voltage (smooth curve) *vs.* time as the LEC is discharged with the system configured to reject negative particles from the MCP and the UDT at -10V.

800V, respectively, while the UDT was allowed to range from negative 100V to positive 100V. Since the electron beam energy was equal to the UEC voltage (V_{UEC}=-500V), in this configuration electrons released from the trap during discharge of the LEC were rejected from the MCP. Positive ions were either accelerated into the MCP for negative UDT voltages or rejected for positive UDT voltages. Figure 4 shows V_{LEC} and the MCP output as a function of time with the UDT at negative 10V. Typical rates of 5000 counts during the 750 μs counting window can be compared to a background counting rate of approximately 1 Hz.

The number of counts due to positive ions was found to decay as a function of time between cessation of electron injection into the trap and LEC discharge with the same time constant ($\sim$30 ms) as that found for the trapped electron lifetime decay. To ensure that the detected signal was not due to ion emission caused by electrons impinging on the grid during trap discharge, measurements of the positive signal appearing at the MCP were made while the full electron beam was allowed to strike the LEC grid. No enhancement above background was seen. Additionally, the trap was reconfigured to dump the electrons in the opposite direction, i.e. to the UEC rather than the LEC, while preserving the same accelerating potential for positive particles. The same positive particle signature was seen.

Finally, although the lifetime would be severely limited by loss to the 50% transmissive grid, it is possible that positive ions were trapped by the negative potential applied to the LEC relative to the positive ring and UDT. This possibility was discounted by discharging the UDT in the same manner that the LEC was discharged during regular operation. No enhancement of counts above background was seen. We therefore conclude that the positive particles arriving at the MCP during trap discharge are ions trapped in a virtual cathode provided by the electron space charge.

In order to determine the total number of trapped ions, one must know the detection efficiency at the MCP. An order of magnitude estimate can be obtained by measuring the ion count rate on the MCP with the electron beam reflexing in the trap and with the MCP and both drift tubes biased to accelerate ions into the MCP. Comparing this measured rate with an expected rate calculated from the known neutral gas density, the energy and density of the beam electrons, and the ionization cross section for H_2 we find an efficiency on the order of 10^{-4}. This is presumably limited by losses to the LEC and LDT as well as by the detection efficiency of the MCP for ions. Losses to the LDT are exacerbated by its length (14 cm) and length-to-diameter ratio (30) compounded by its location in the fringe of the magnetic field at approximately half the central field value of 2T. Five-thousand ions collected at the MCP during the counting window then correspond to on the order of 10^7 total trapped ions with a density on the order of 10^9 cm^{-3}. Although this is only an order of magnitude estimate, one can compare this to the average electron density in the trap volume of 3×10^9 cm^{-3} indicating that f_i is on the order of 1.

Future work will concentrate on directly ascertaining the strength of the virtual cathode and increasing the ion well depth. Direct measurement of the ion well depth may be accomplished by measuring the Stark splitting of the optical lines of hydrogen [14] caused by the space charge of the electron plasma. Producing measurable splitting and increasing the overall strength of the cathode will, obviously, require greater electron density which in turn results from greater electron well depth. This necessitates raising the endcap voltages. We have conducted tests on some components of the present system to 75 kV in the presence of a 1 T magnetic field and have operated an electron beam in 1 T at 40 kV with a slightly modified geometry from the one used in the above reported measurements. We have also initiated investigations into different anode void shapes to study ion focusing.

We are grateful to M. H. Holzscheiter, L. Chacón, F. L. Ribe, L. S. Schrank for helpful conversations. This work was supported by the Office of Fusion Energy Sciences.

REFERENCES

*. Present address: Archimedes Technology Group, 5405 Oberlin Drive, San Diego, CA 92117.
1. L. S. Brown and G. Gabrielse, Rev. Mod. Phys. **58**, 233 (1986).
2. L. Brillouin, Phys. Rev. **67**, 260 (1945).
3. T. B. Mitchell, M. M. Schauer, and D. Barnes, Phys. Rev. Let. **78**, 58 (1997).
4. D. Barnes, T. Mitchell, and M. Schauer, Phys. Plasmas **4**, 1745 (1997).
5. W. Elmore, J. Tuck, and K. Watson, Phys. Fluids **2**, 239 (1959).
6. R. Hirsch, J. Appl. Phys. **38**, 4522 (1967).
7. R. Nebel and D. Barnes, Fusion Tech. **34**, 28 (1998).
8. D. Barnes and R. Nebel, Phys. Plasmas **5**, 2498 (1998).
9. M. Levine *et al.*, Physica Scripta **T22**, 157 (1988).
10. M. Levine *et al.*, Nuc. Inst. Meth. Phys. Res. **B43**, 431 (1989).
11. P. Beiersdorfer, L. Schweikhard, K. Widman, EBIT Program Bi-Annual Report 1996-1997, 104 (1998).
12. M. Schauer, K. Umstadter, and D. Barnes, AIP Conf. Proc. **498**, 425 (1999).
13. D. C. Barnes, M. M. Schauer, K. R. Umstadter, L. Chacon and G. Miley, Physics of Plasmas **7**, 1693 (2000).
14. H. Bethe and E. Salpeter, *Quantum Mechanics of One- and Two-electron Atoms* (Springer-Verlag, New York, 1957), p. 228.